Estimation of vorticity from fibrous calcite veins, central Maine, USA

H.A. Short *, S.E. Johnson

Department of Earth Sciences, 5790 Bryand Global Sciences Center, University of Maine, Orono, ME 04469-5790 USA

Abstract

An estimate for the vorticity of a mid-Paleozoic deformation was made using deformed and/or rotated calcite veins as natural vorticity and shear-strain gauges in a northern part of the U.S. Appalachians. The spatial distribution of extended, shortened, and shortened-then-extended elongate fibrous calcite veins in limestone layers were used to construct a Mohr circle for the position gradient tensor **H**, from which vorticity and flow parameters were calculated. The amount of rotation of large axial-ratio fibrous calcite veins in quartz-phyllite-layer boudin necks and linear veins in limestone layers were used to calculate shear strain as a check on flow parameters calculated from the distribution of deformed veins. These analyses demonstrate that the D_3 phase of deformation was characterized by a mean kinematic vorticity number of 0.67. The existence of a non-coaxial fabric defined by reactivated foliation and dextral asymmetric folds is also established. Age constraints suggest that this non-coaxial deformation in eastern central Maine began early in the Devonian and continued at least through regional peak metamorphism. This study represents the first quantitative assessment of the vorticity of Devonian deformation in Maine, and the results suggest that a transpressional tectonic model is appropriate for the area at that time.
© 2006 Elsevier Ltd. All rights reserved.

Keywords: Vorticity; Fiber veins; Progressive deformation; Maine; Mohr circles

1. Introduction

An important goal of structural geology is to reconstruct the deformation history of discrete volumes of rock from the geometry and orientation of fabric elements (Lister and Williams, 1983). The resulting data can be used for regional kinematic analysis, and can be integrated with petrologic, geochemical, and numerical modeling studies to gain a better understanding of crustal dynamics. Quantitative determination of the vorticity is extremely valuable when attempting to reconstruct a deformation because it describes the degree of non-coaxiality of flow, or the relative amounts of pure versus simple shear, and helps to define the kinematic reference frame during orogenesis. Many workers have developed theoretical techniques to determine strain and vorticity in deformed rocks (Passchier, 1987, 1990a; Simpson and De Paor, 1993; Tikoff and Teyssier, 1994). However, few studies have attempted to quantify strain parameters and vorticity in naturally deformed rocks (Wallis, 1992; Simpson and De Paor, 1997; Bailey and Eyster, 2003). Vorticity can be defined as the ratio of pure to

simple shear components of deformation (Means et al., 1980). The kinematic vorticity number, W_k, is a dimensionless number that describes this quality of flow, where pure shear is described by $W_k = 0$, and simple shear is described by $W_k = 1$. General shear is the term used for flows intermediate between the pure and simple shear end members, in which $1 > W_k > 0$. Although general shear appears to be the rule in many deformations and not the exception, theoretical strain compatibility problems arise in discrete high-strain zones of general shear (Simpson and De Paor, 1993). However, the pure and simple shear components of a general shear deformation are compatible where the wall rock is deformable, where volume change is able to occur along non-parallel shear zone boundaries, and/or in cases where the high-strain zone is separated from the wallrock by a fault (Simpson and De Paor, 1993).

Regional deformation in eastern central Maine, USA, is characterized by NE-trending symmetric folds and foliation, and transcurrent structures associated with distributed dextral shear centered around the orogen-parallel Norumbega fault system (Fig. 1). Collectively, these structures have traditionally been interpreted as evidence for two separate phases of regional mid-Paleozoic deformation: initial orthogonal convergence and predominantly coaxial strain, followed by later, oblique convergence and major (West and Hubbard, 1997) or minor (Osberg, 1988; Tucker et al., 2001) non-coaxial strain. The amount, significance, and duration of the non-coaxial
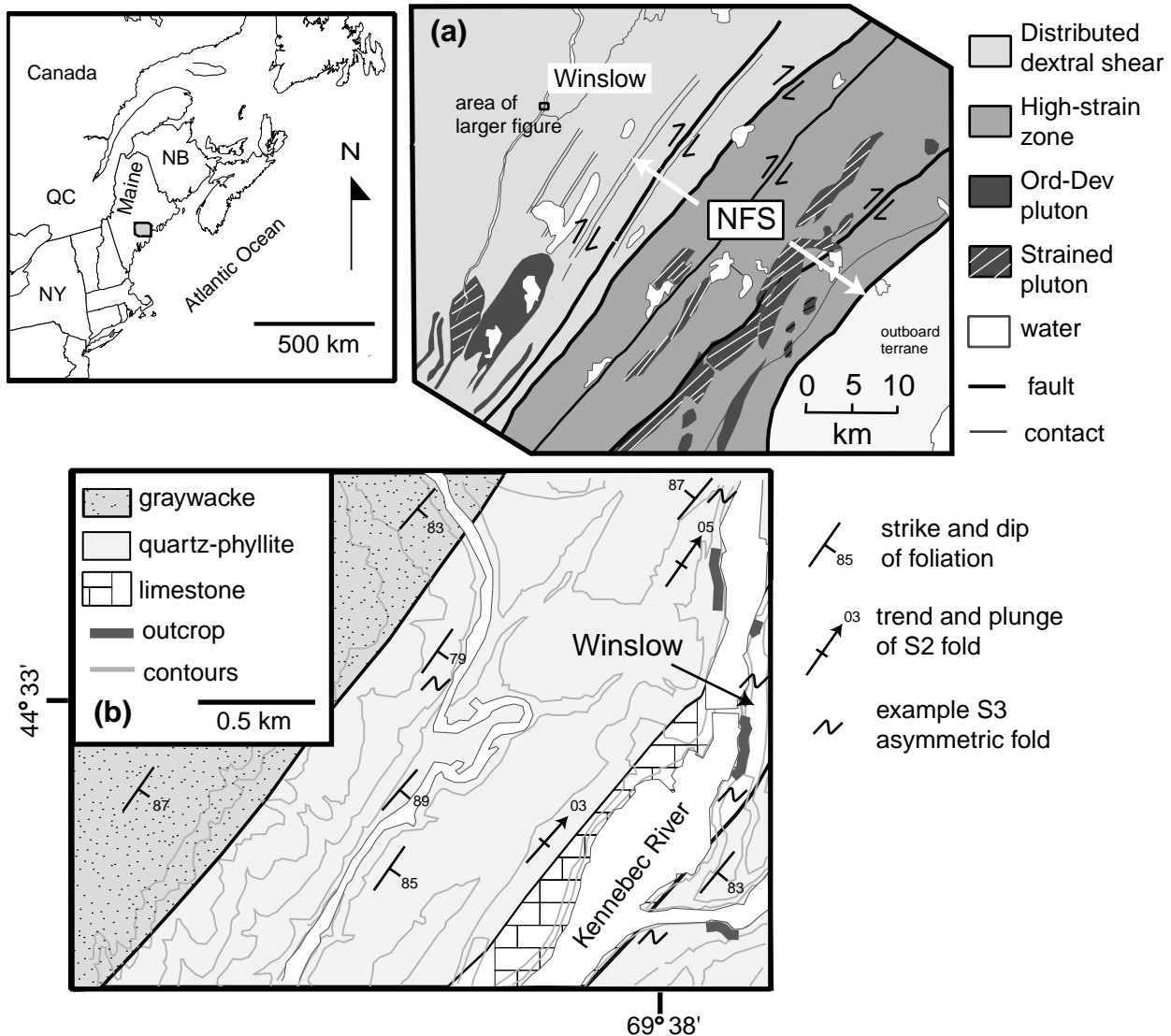
Fig. 1. Location and geological map of the Winslow area, eastern central Maine, USA (inset). (a) Regional structure map of eastern central Maine showing position of the study area in the broader zone of distributed dextral shear. Boundary between the high-strain and distributed shear zones is approximate. NFS = Norumbega fault system. (b) Geologic map of the Winslow area after Osberg (1968), highlighting locations of outcrops used in this study.

strain are unclear, and no attempts have been made to quantitatively document or estimate this strain. In this paper, the structures preserved in an outcrop of the Waterville Formation in Winslow, Maine, are used to estimate vorticity during Devonian-aged deformation. The outcrop is located within a broad zone of distributed dextral shear on the west side of the dextral strike-slip fault system (Fig. 1). Any potential general shear strain incompatibilities are avoided in this study because the rocks analyzed *are* the deformed wallrock. Variably oriented and deformed fibrous calcite veins in limestone are analyzed using the distribution of deformed lines and the Mohr circle for position gradient tensor **H**, as described by Passchier (1988, 1990a,b). We use the results to determine vorticity, the kinematic dilatency number *A* (Passchier, 1990a), the finite strain ratio, and orientations of the finite strain axes. As a check on the flow parameters determined with this method, large-axial-ratio fibrous calcite veins in boudin necks of competent layers are used in addition

to longitudinal, layer-spanning calcite veins in limestone to generate average shear strain estimates for each rock type. Although isolated outcrop-scale analyses have inherent limitations, they allow useful inferences about the larger-scale deformation. Quantitative determination of the amounts of pure and simple shear, and limits on the timing of the non-coaxial deformation from a well-exposed area in eastern central Maine allows for a better understanding of the significance of non-coaxial strain and transpression in the northern Appalachians.

2. Geologic setting

Central Maine consists of a series of NE–SW-striking belts of rock with similar deformational and metamorphic histories, though deformation intensity and metamorphic grade generally increase across regional strike from west to east, toward the Norumbega fault system and its broader distributed shear zone

(Osberg et al., 1985; West and Hubbard, 1997; Tucker et al., 2001; West et al., 2003). The study area consists of a series of large outcrops of the middle limestone unit of the Waterville Formation on the east bank of the Kennebec River in Winslow, Maine (Fig. 1). The Waterville Formation is part of the Central Maine sequence, a package of variably-metamorphosed metasedimentary rocks of Early Silurian age that are interpreted to have been derived from a volcanic terrane to the west, and deformed and metamorphosed during the Late Silurian through Devonian (Osberg, 1988). The 5–25-cm-thick beds of grey limestone of the Waterville Formation are interlayered at this locality with beds of quartz-mica phyllite and quartz-phyllite that are 1–15 cm thick. The limestone consists of fine-grained calcite with sparse flakes of ilmenite. Very fine-grained micas and <2 mm bands of quartz define the matrix foliation in the limestone, where visible. According to previous workers (Osberg, 1988; Bickle et al., 1997) these outcrops are located within the chlorite zone of regional Devonian metamorphism (380 Ma; Tucker et al., 2001). Chlorite is present along the boundaries between the matrix and calcite veins in the quartz-mica phyllite layers, but never in the matrix. The presence of $\sim$0.4 mm biotite grains in the quartz-mica phyllite layers suggests that these rocks belong in the biotite zone.

2.1. Coaxial and non-coaxial structures

The outcrop in Winslow is dominated by NE-trending, upright isoclinal folds that plunge 0–35° NE. The folds are approximately 5–10 m in amplitude and are associated with a major regional folding event, F_2 (Osberg, 1968, 1988; Tucker et al., 2001). The existence of an F_1 folding event is postulated on the basis of facing directions of F_2 folds that are inconsistent with fold geometry (Osberg, 1968, 1988), although direct evidence for the F_1 folding as an event distinct from F_2 was not observed in this study. Axial-surface-parallel foliation associated with F_2 folding is approximately parallel to bedding (Osberg, 1968, 1988). Bedding can be measured at the boundaries between limestone and quartz-phyllite layers. Compositional variation in the quartz-phyllite layers appears to parallel these contacts, but at least two later foliations are subparallel to the compositional layering, so it is difficult to determine if the layering is primarily sedimentary or tectonic. Foliation in the quartz-mica phyllite layers is defined by mica-rich bands, and the latest fabric is commonly refracted across the quartz-rich layers. The dominant matrix foliation in the limestone portions of the F_2 fold limbs commonly occurs at a 10–20° angle to axial traces (Fig. 2), transecting the F_2 folds. This foliation is associated with abundant dextrally-rotated veins in both the limestone and quartz-phyllite layers, and for this reason we define it here as a distinct, non-coaxial foliation, S_3 (Table 1). S_3 and associated structures can be traced NW for $\sim$75 km where their intensity diminishes, and east through the rocks of the Norumbega fault system where they are associated with higher strain. A locally developed cleavage typically strikes 0–10° and up to $\sim$25°, deforms S_2, F_2, and commonly S_3. The cleavage parallels the axial surfaces of locally-developed open, steeply-plunging, eastward-verging asymmetric folds (F_3) that also deform S_2 and S_3 foliations and F_2 fold hinges. We interpret this late cleavage and asymmetric folds as having formed during the same progressive non-coaxial deformation as S_3, because (1) there is no evidence for a regional or local E–W shortening event, and (2) the asymmetric folds trend more northeasterly as the more
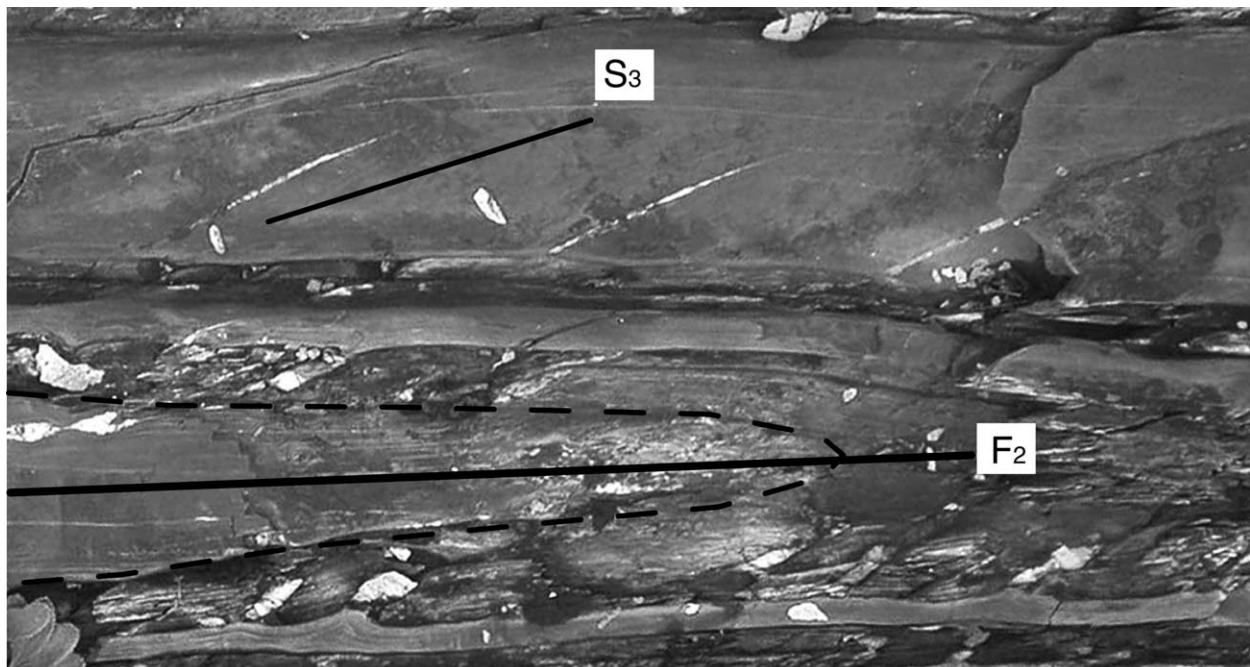

Fig. 2. S_3 foliation at an angle to S_2 axial-surface-parallel foliation. Note that fibrous boudin-neck veins are inclined to the right (dextral sense) on both limbs of the F_2 fold.

Table 1
Summary of the structures and deformation events for eastern central Maine. Structures are listed in relative chronological order from top (earliest) to bottom (latest)

Deformation	Structures and events	Notes
D_1 and D_2 (predominantly coaxial?)	Upright, $\sim 40°$-trending F_2 folds and S_2 axial surface-parallel foliation	Folds are symmetric and dominant in west-central Maine
D_3 (dextral non-coaxial)	Attenuation of F_2 fold limbs, boudinage and fibrous calcite vein formation in the quartz-phyllite layers; calcite veins form in limestone layers as fracture fill	Most veins opened perpendicular to the maximum instantaneous shortening axis at ~ 313–$325°$ NW, and perpendicular to bedding; some opened inclined to bedding
	S_2 re-activated and slightly re-oriented to ~ 30–$40°$ NE, forming the dominant fabric in the area (S_3)	Portions of calcite veins in limestone are dissolved by S_3 formation
	Boudin-neck fibrous veins rotated between 20 and $50°$ in a dextral sense, forming flanking folds; asymmetric F_3 shear folds and cleavage form in a N–S orientation and rotate in a dextral sense through progressive deformation	S_3 foliation and structures constitute a broad zone of distributed dextral general shear
		D_3 active by 399 Ma
D_3 (?) Norumbega fault system	Discrete, high-angle, orogen-parallel dextral strike slip faults	Active through the Carboniferous (?)

intensely-deformed shear zone rocks are approached (Fig. 1). These observations imply a genetic relationship between the regional S_3 foliation and the asymmetric folds and cleavage.

Quartz-phyllite layers in the Waterville Formation are heterogeneously boudinaged or fractured as a function of layer thickness and the thickness of adjacent limestone layers. Layers less than ~ 4 cm thick tended to stretch and deform plastically rather than form boudins, especially if the surrounding limestone layers were relatively thick. Layers between ~ 4 and ~ 6 cm thickness formed boudins with rectangular, equant, circular, and irregularly shaped fiber veins filling boudin necks. The long axes of boudin-neck veins presently trend between 350 and $10°$, and adjacent asymmetric folds are interpreted here as having developed as the veins rotated clockwise during progressive non-coaxial deformation (Fig. 3). These n- and s-type flanking folds (Passchier, 2001) in the boudin segments are locally intensely developed, particularly where F_3 asymmetric folds are present. Layers approximately 7 cm thick or more formed fractures 2–5 mm wide with fiber vein fill that can commonly be traced into the limestone layers, where the veins thin to barely visible lines and form a smaller angle with bedding. These fractures constitute a localized fabric that cuts across the hinges of the F_2 folds at a moderate angle and strikes N–NE, varying between 0 and $28°$ (Fig. 4). The fact that the fractures are filled with vein material implies that this fabric is not a cleavage, as the veins are not likely to open in the direction of maximum compression. Instead, these tiny fiber-vein-filled fractures formed under extension at the same time as the quartz-phyllite layer boudinage, and rotated with them in a dextral sense.

3. Fibrous calcite veins

Two types of fibrous calcite veins occur in the Waterville Formation at this location, one as fill in the necks of boudinaged quartz-phyllite layers, and the second as variably oriented and deformed, fibrous and equant calcite veins in the limestone layers. The boudin-neck and limestone veins are used to estimate the finite shear strain and flow parameters, respectively, during the D_3 stage of a progressive deformation.

Fiber veins in the boudin necks can be traced into fibrous veins in the limestone and vice versa (Fig. 3), suggesting that their formation was contemporaneous.

3.1. Limestone vein origin and morphology

Veins in the limestone layers of the Waterville Formation have moderate to large aspect ratios of 8–60, and are generally thin (~ 5 mm) and long (4–30 cm). Vein fill is varied, and some veins and sections of veins contain fibrous and/or equant calcite. A median line of wallrock is visible in some veins in outcrop (Fig. 5), suggesting that portions of some limestone veins may contain antitaxial fibers, and may have opened under the force of crystallization (Means and Li, 2001; Wiltschko and Morse, 2001; Bons and Montenari, 2005). However, in thin section, limestone veins consist of strongly twinned equant calcite, and no fiber ghosts were observed, suggesting that most veins in the limestone layers originated as fracture-fill, perhaps with vein sections oblique to the principal opening direction forming antitaxial fibers. No fibrous calcite growth or displacement parallel to the fracture walls was observed in outcrop or thin section, so the veins are not shear fractures (Bons, 2000). The calcite veins in limestone most likely originated as Mode I fractures that opened in the direction of maximum instantaneous extension through longitudinal fracturing (Engelder, 1987). Limestone veins extend across entire layers, and commonly consist of boudinaged, shortened, and/or shortened-then-boudinaged sections. Initial orientations of straight extended veins can be reconstructed and are close to layer-perpendicular when visually back-rotated so that the curved foliation adjacent to the vein is made straight and continuous with the dominant foliation. Such layer-spanning veins are used to estimate shear strain in Section 5. The veins in limestone described here very rarely intersect each other, suggesting that they all formed at approximately the same time and by the same mechanism. Irregularities in fracture shape and initial orientation allowed different veins and sections of veins to experience different stretch and rotation histories during progressive deformation, with some back-rotating against
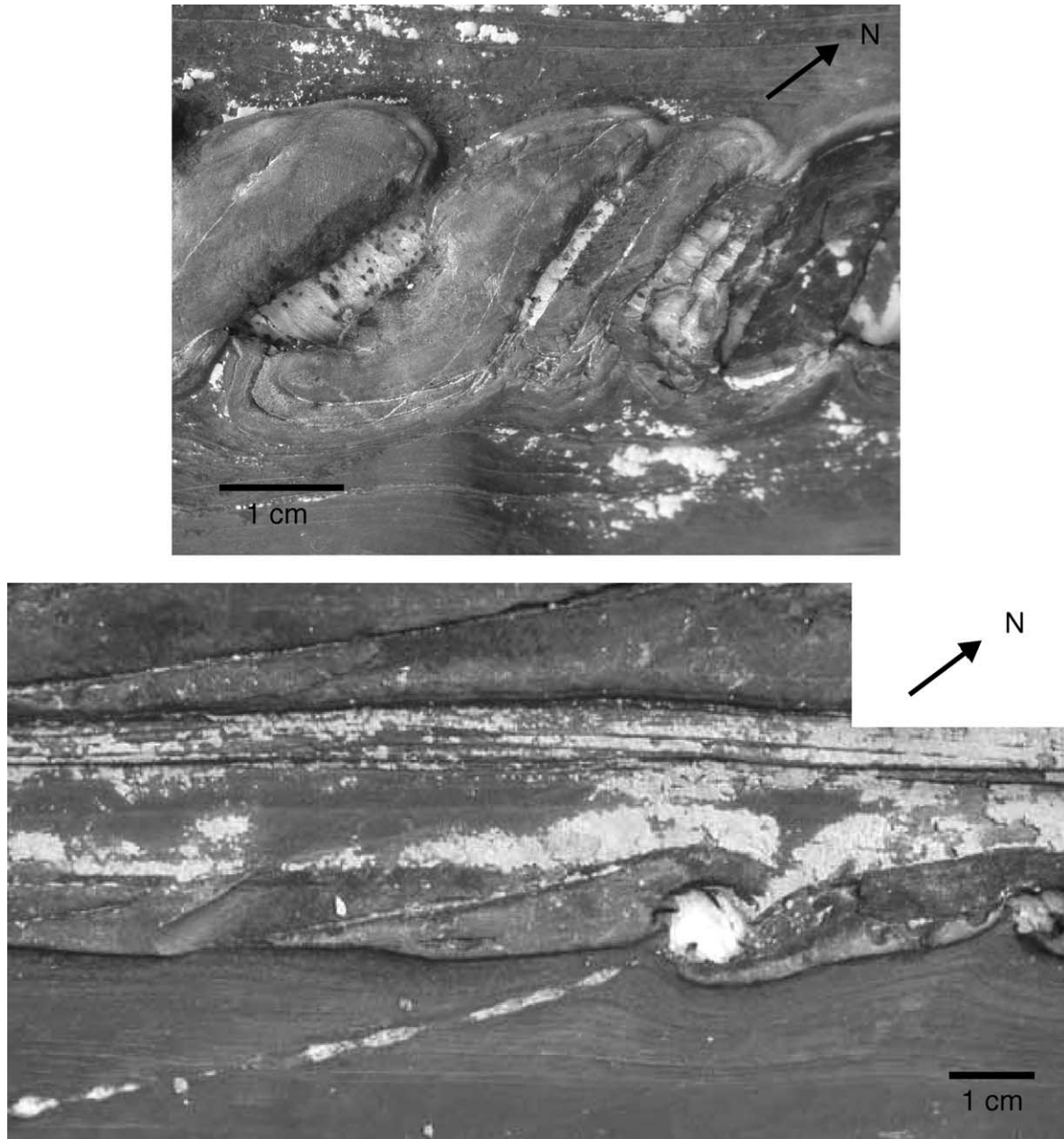
Fig. 3. Calcite fiber vein fill in the necks of boudins. The rock experienced a non co-axial deformation after boudinage, hence the folding of the boudin segments around the fiber veins and rotation of the veins. A more common rectangular morphology is shown at the top, and a less common circular vein is shown at the bottom. Note that an extended vein in the limestone can be traced directly into a boudin-neck vein. Vein fibers were initially parallel and continuous with the foliation in the boudin segments.

the bulk flow, resulting in a ∼180° spread of final orientations (Fig. 6). An analysis of these different stretch histories forms the basis for the estimate of vorticity and flow parameters for this progressive deformation.

Equant calcite grains in veins in limestone are twinned, and larger grains have deformation twins, curved twins, and show undulose extinction. Deformed and intersecting calcite twins suggest that a *minimum* temperature of 250 °C was reached during the deformation of those veins (Burkhard, 1993). Larger calcite grains show evidence for grain boundary migration recrystallization (GBMR) in the form of irregular grain boundaries, implying that temperatures reached >300 °C

during D$_3$ deformation (Vernon, 1981; Burkhard, 1993). Cuspate, irregular boundaries between calcite fibers in boudin-neck veins in quartz-phyllite layers also suggest active GBMR (see below). Buckled veins are commonly segmented, and the matrix foliation is defined by tiny opaque minerals concentrated between the segments in a matrix of fine-grained carbonate (Fig. 7). In some instances, the fold segments and insoluble minerals are pulled apart, and in others the segments are pushed back on each other and the insoluble minerals and matrix foliation are folded around the converging segments. These morphologies and their implications are discussed further in Section 4.3.
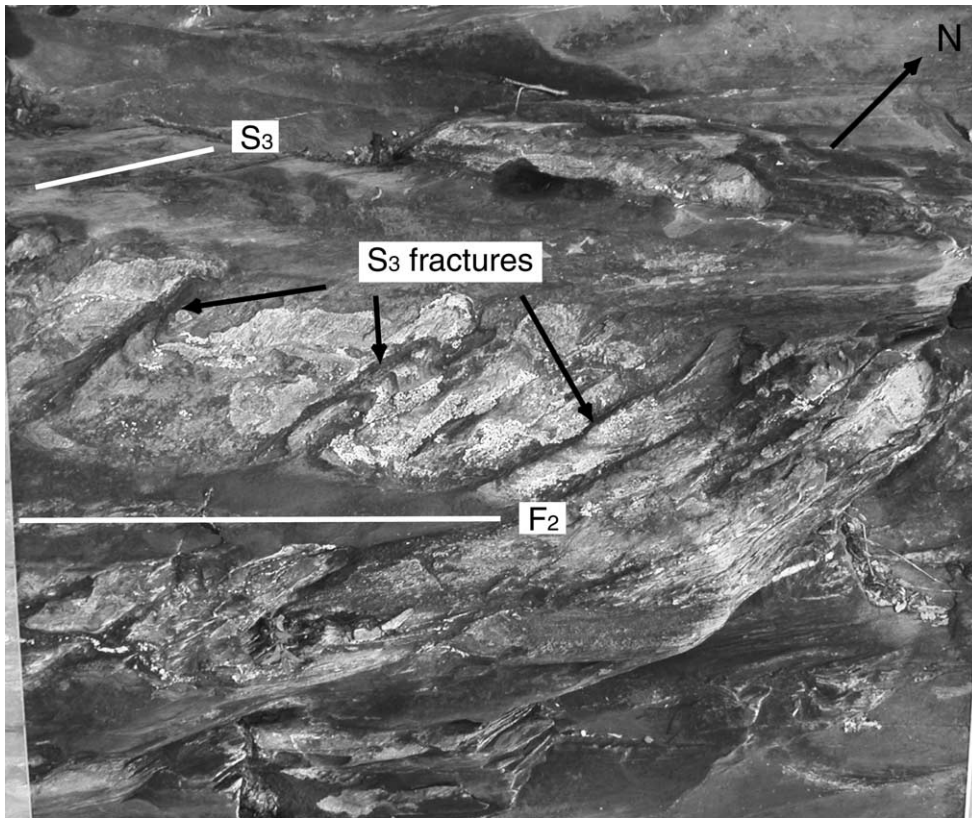
Fig. 4. A series of fiber vein-filled fractures in the competent quartz-mica phyllite forming a fabric that cuts an F_2 fold hinge. Note how the fabric is at an angle to both the F_2 axial trace and the S_3 foliation in the adjacent limestone.

3.2. Boudin-neck vein origin and morphology

Quartz-phyllite layer boudin-neck veins are typically ∼0.5–1 cm wide and 1–2.5 cm long. Individual original fibers have aspect ratios of 20–30, and have similar shapes showing little or no growth competition. These fiber veins show no distinct original median line or zone, no inclusion bands, and undeformed fibers are commonly straight and optically continuous from one side of the vein to the other. However,

a few veins display sharp, ∼90° curves in fiber shape at the NE and SW corners of the veins while retaining optical continuity of the fibers, indicating that growth was antitaxial (Fig. 8a) (Durney and Ramsay, 1973). The youngest fiber growth is concordant with late cleavage nearly parallel to the vein wall, indicating that calcite fibers were still growing during the later stages of non-coaxial deformation. Boudin-neck fiber veins are also surrounded by a thin quartz selvage typical of antitaxial calcite fibrous veins (Williams and Urai, 1989; Hilgers and

Fig. 5. Calcite fiber vein in limestone with median line visible. S_3 foliation is NE–SW, visible as faint white lines.
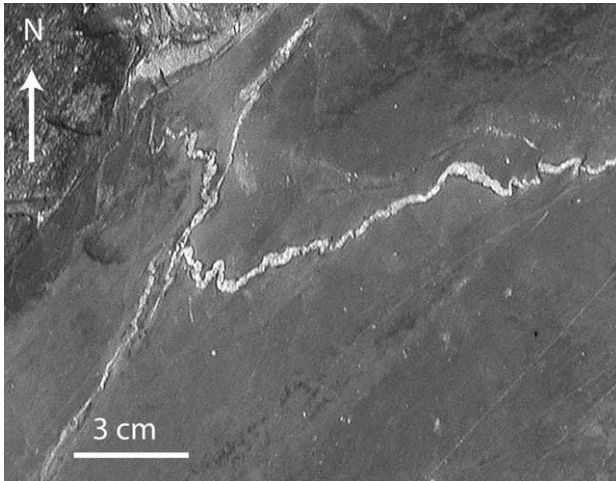
Fig. 6. Photo of limestone layer with fibrous calcite veins. Each vein experienced a different stretch history, which corresponds to its present shape and orientation.

Urai, 2002) (Fig. 8b), and mica grains in the selvage form curved paths connecting matrix foliation with calcite fibers. Antitaxial veins are formed by growth of fibers simultaneously on the two opposite vein/wallrock surfaces while mechanical continuity between those materials is maintained, although the dynamic and geochemical conditions under which they form remain unclear (Means and Li, 2001; Wiltschko and Morse, 2001; Bons and Montenari, 2005). The relatively small vein aspect ratios (1.5–3; ∼1 for circular veins), the irregularity of the boudinage (straight fractures to fish-mouth) and corresponding fiber vein shapes, and the absence of less-competent limestone material in the boudin necks suggests that antitaxial vein growth was coupled with the boudinage of the quartz-phyllite layers. Jagged wallrock protrusions into the fiber veins parallel to fibers are common, and would not have occurred if the quartz-phyllite layers had simply boudinaged in the absence of vein fill. Fluid pressure must have been high enough for the calcite fiber veins and quartz selvage to grow as the boudin necks opened, maintaining contact with the wallrock. Calcite fibers in most boudin-neck veins began

their growth at right angles to the vein walls, indicating that the veins' long axes initially formed perpendicular to the initial direction of maximum extension (Bons and Montenari, 2005). However, uncommon boudin-neck veins with long axes inclined 10–25° to bedding, but with fibers still parallel to and continuous with the dominant foliation, suggest that some boudinage may have initiated somewhat later during the D_3 non-coaxial deformation. Such veins were avoided when measuring the amount of rotation of the long axes of boudin-neck fiber veins in Section 5.

What appear to be median lines in many of the boudin-neck fiber veins at outcrop scale are, on closer inspection, lines down the long axis of the vein where fibers that dynamically recrystallized in response to folding meet at an angle (Fig. 8b). Note that in Fig. 8b, fibers are progressively more bent as the bottom of the vein is approached, and a pseudo-median line appears half-way down the vein where original single fibers have 'split' into two. This fiber geometry cannot represent the original growth trajectory of the fibers, as it would require the antitaxial vein to open in two non-parallel directions. Where fibers are curved into C or S shapes, undulose extinction perpendicular to fiber long-axes is present (Fig. 8c), indicating that, where curved over broad arcs, the fibers are indeed folded and do not reflect progressive change in the orientation of the vein opening trajectory during deformation (Williams and Urai, 1989). Further deformation of the boudin-neck veins is evident by irregular and cuspate dynamically recrystallized grain boundaries between the fibers (Fig. 8d). In these cases, sliding parallel to fibers appears to have occurred, as bundles of calcite fibers are slightly offset relative to each other in the quartz selvage (Fig. 8d).

4. Distribution of deformed lines and estimates for W_m, sense of shear, finite strain, and area change of flow

4.1. Terminology

The following terminology refers to two-dimensional flow and deformation, and is used in the remainder of this paper.
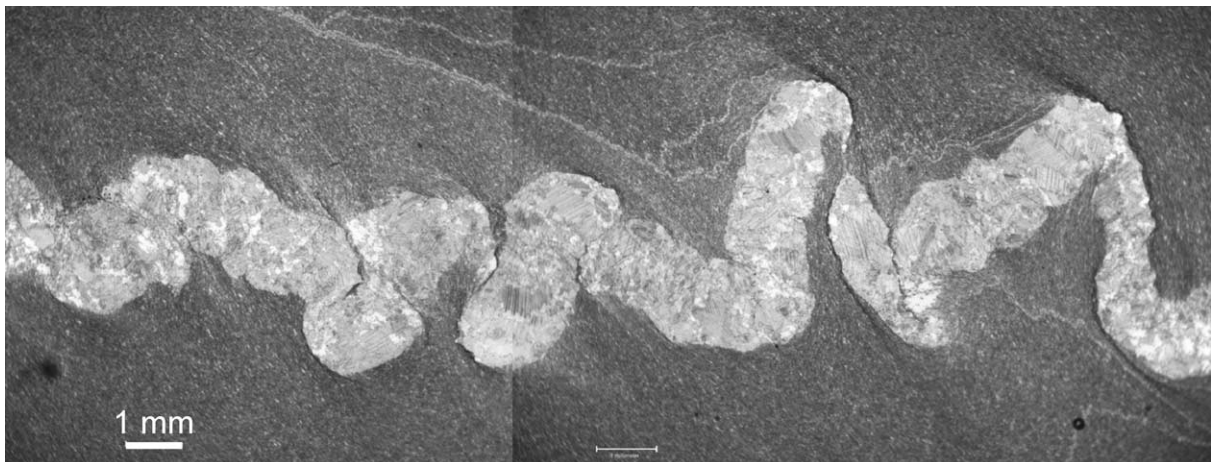

Fig. 7. Composite photomicrograph of shortened calcite vein in limestone. Note the thinning of portions of the folds parallel to the S_3 matrix foliation through boudinage and pressure solution. The left-hand side of the figure shows vein segments impinging on each other due to continued shortening.
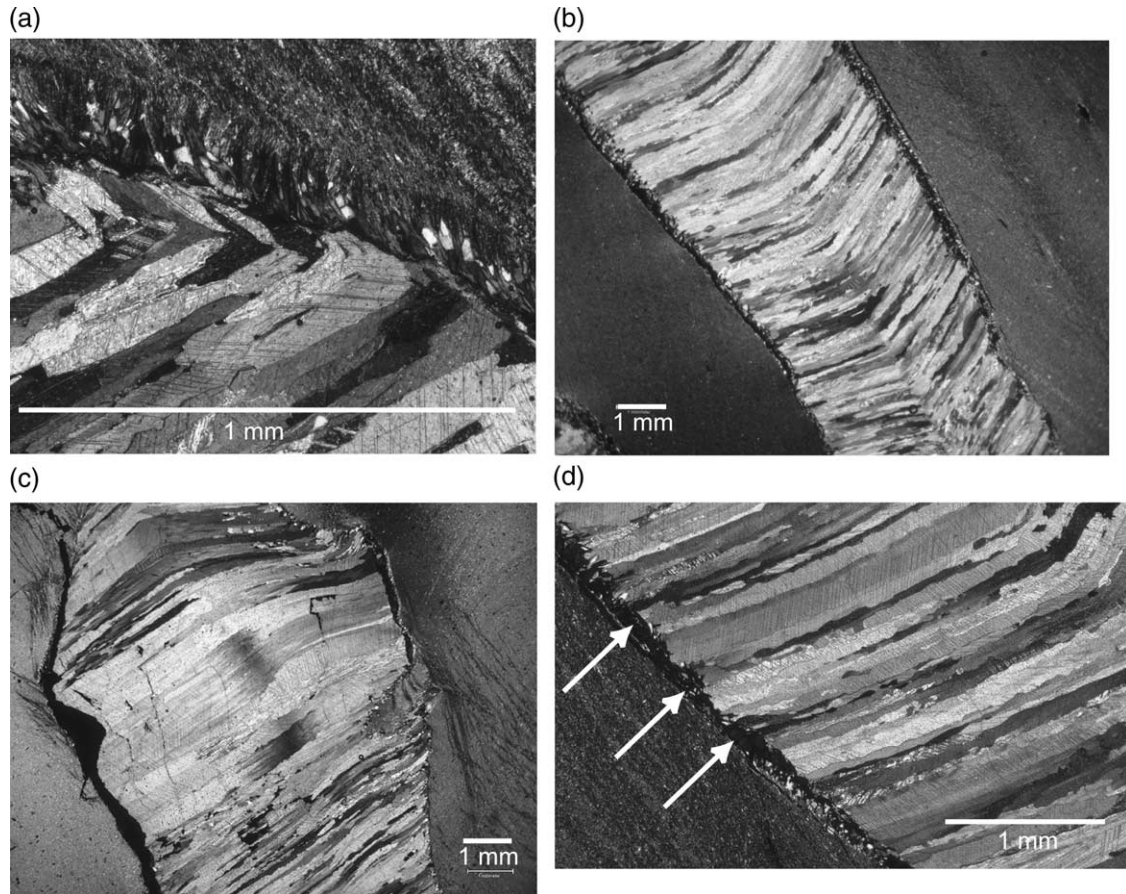
Fig. 8. Photomicrographs of boudin-neck fiber veins in quartz-phyllite layers. (a) Optically continuous calcite fibers with a sharp change in growth direction at the vein-selvage interface, indicating antitaxial growth. (b) The formation of a median line through the recrystallization of calcite fibers. Fibers are continuous and extend across the vein at the upper left, and progress to separate calcite grains that meet in the middle, forming pseudo-median line. (c) Undulose extinction perpendicular to fiber long axes, indicating deformation of fibers. (d) Dynamically recrystallized calcite fibers indicated by irregular, cuspate grain boundaries, particularly where fibers are offset parallel to each other (note the stair-step morphology of groups of fibers in quartz selvage (arrows)).

Flow refers to instantaneous homogeneous flow at a particular moment during progressive deformation. We assume steady-state flow, in which (1) flow parameters remain unchanged during the deformation, and (2) the orientations of the flow apophyses (see below) remain fixed with respect to the external reference frame. Finite deformation refers to the final deformation state only (Passchier, 1990a). W_m is the mean kinematic vorticity number, and is typically what is determined in vorticity studies using naturally deformed rocks, as the total strain is what is recorded. Flow apophyses, also known as the eigenvectors of flow, represent lines of no rotational strain with respect to the instantaneous stretching axes (Ramberg, 1975; Passchier, 1988). All material lines rotate toward the extending line of no instantaneous angular velocity, or the extensional flow apophysis, during progressive deformation. This line is also commonly referred to as the fabric attractor (Passchier and Trouw, 1996). Mohr circle construction is a convenient way to translate measurements such as the stretch and rotation of material lines into tensors (Means, 1982; De Paor, 1983). The Mohr circle for **H** is a representation of the Eulerian or spatial tensor relating particle positions in the deformed state back to their positions in the undeformed state, also called a position gradient tensor (Passchier, 1990b). The tensor **H** is defined by

the equation:

$$x = \mathbf{H} \cdot x'$$ (1)

where x and x' are the Cartesian coordinates of material points in the undeformed and deformed states, respectively. Mohr circles are constructed using a Cartesian coordinate system in Mohr space, and the polar coordinates for a point on the Mohr circle for **H** represent the stretch and rotation of a material line in real space (Means, 1982; Passchier, 1988). Because of this quality of the Mohr circle for **H**, it is sometimes said to be constructed in stretch space.

4.2. Methodology

In progressive deformation, material lines will rotate toward the extensional flow apophysis, during which the material lines may undergo shortening, extension, or both. Material line markers such as cross-cutting dikes and veins have been used to determine finite strain and sense of shear in deformed rocks (Talbot, 1970; Passchier, 1986), based on the geometric distribution of boundaries between sets of material line markers with similar stretch histories. The advantage is that this method relies on the orientations of lines, which can be

fairly accurately measured, without actually determining the stretch along the markers, which is a considerably less precise procedure. The method is based on the facts that: (1) material lines that experienced similar stretch histories will have a restricted orientation range, and when plotted as lines on a stereographic projection they cluster in arcuate sectors; and (2) the angle between lines of no finite longitudinal strain in any plane is a function of the strain ratio. The boundaries between material line sectors correspond to the orientations of material lines that lie parallel to lines of no instantaneous longitudinal strain at the onset of deformation and at the final increment of deformation (Fig. 9) (Passchier, 1990a). Sectors of shortened (s) veins and extended (e) veins will always be separated by sectors of veins that have first been shortened-then-extended (se) because the orientations of material lines parallel to the initial lines of no instantaneous longitudinal strain will rotate toward the extensional apophysis during deformation, creating the se-sectors. Consequently, the size and shape of the material line sectors in real (geographical) space depends on the vorticity and area change rate of the flow (Passchier, 1990a,b). In pure shear, the two (se) sectors would be equal in shape and size because approximately the same number of veins would rotate in both the clockwise and anti-clockwise directions. In simple shear, only one (se) sector would develop because all material lines would rotate in one direction. In the case of general shear, two unequal (se) sectors develop with the majority of material lines rotating with the bulk flow, and fewer back-rotating due to a high initial angle to the direction of maximum shortening.

If the orientations in geographical space of deformed material lines with similar stretch histories is known or can be determined, then the method described by Passchier (1990a) of Mohr circle construction for the position gradient tensor **H** in stretch space can be used to determine estimates for all of the

parameters of finite deformation. The method is applicable only if the deformation has accumulated by approximately steady state homogeneous flow, on the scale of the surface area for which the analysis is carried out (Passchier, 1990a,b). Although deformation in eastern central Maine and even within the outcrop at Winslow is not homogeneous, one major advantage of the study area is that there is 100% exposure of the Waterville Formation and deformed veins for several hundreds of meters, so data location is controlled and structural relationships are readily observed. The complete exposure and repetitive nature of the limestone/quartz-phyllite layering has allowed us to evaluate the compositionally controlled partitioning of strain in the outcrop and to work from the assumption that the deformation analyzed in each of the two layers is relatively homogeneous. Foliation is near-vertical to steeply-SE-dipping, and the surface of the outcrop is near-horizontal to shallowly-dipping NW, so all veins were observed approximately in the XZ plane of the finite strain ellipsoid, approximately perpendicular to the Y-axis and the vorticity vector.

4.3. Determination of the distribution of deformed veins

The orientations of over 300 calcite veins in the limestone layers of the Waterville formation were measured and categorized as (s), (e), and (se) veins in the field. A majority of veins were also recorded with oriented digital photographs for a further check on consistency in categorization. The determination of the boundaries between sectors of deformed veins is a critical step in this method for the determination of flow parameters (Passchier, 1990a). The criteria used for determining if a vein belonged in an (s), (e), or (se) sector were as follows: (s) veins must be obviously folded and show no sign of extension such as thinning or unfolding; (e) veins must be
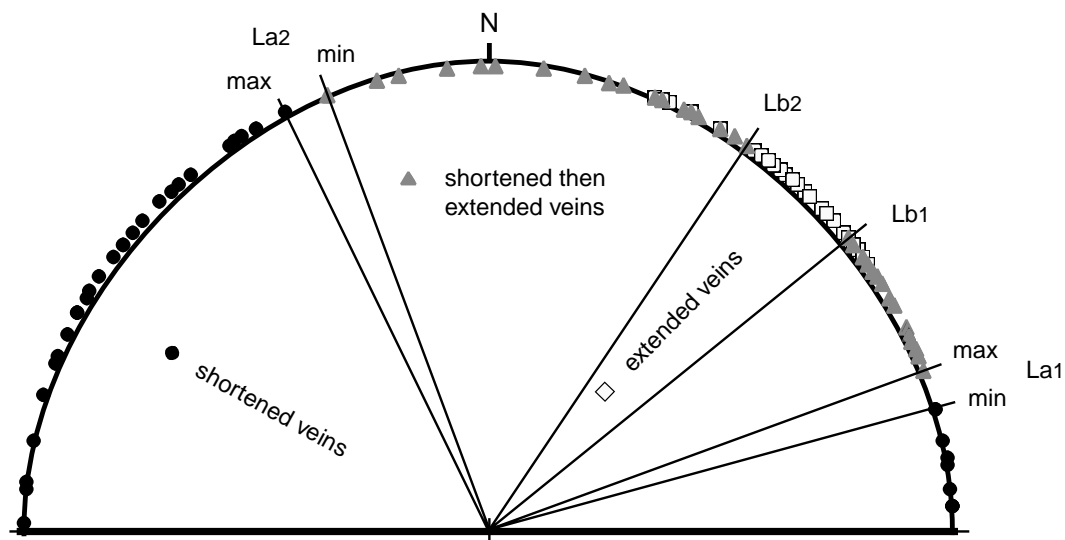

Fig. 9. The distribution of deformed veins with similar stretch histories plotted as points in a radius from a central point according to their orientations in geographic space, after Passchier (1990a). *La–Lb* lines are lines of no instantaneous stretching that separate the sectors of veins with different stretch histories. The unequal size of the (se) sectors indicates that the deformation was dextral non-coaxial. The angles between these sectors were used to construct maximum and minimum Mohr circles for the position gradient tensor **H**, to determine the parameters of flow for the D$_3$ deformation.

obviously boudinaged or thinned, without obvious fold segments; and (se) veins consist of veins that: (1) retain a folded morphology but have thinner, elongated limbs on one side, subparallel to foliation, or (2) have been clearly boudinaged after folding with the boudin segments preserving a folded morphology (Fig. 10). A special class of dissected (se) veins was distinguished from the two types described above because of their probable deviant behavior under these flow conditions. These dissected (se) veins experienced complete dissolution of fold limbs parallel to the S_3 fabric while in the shortening sector, resulting in a line of individual vein segments that then rotated as individual rectangular clasts in the matrix rather than as a continuous material line. Segmented lines only occur near the (se) sector in which the material lines rotated anti clockwise, against the bulk rotation, because their initial orientation was at a high angle to the direction of maximum instantaneous shortening (Ghosh and Ramberg, 1976). Depending on the segment's orientation in the extension sector after dissection, each segment rotated clockwise, anti-clockwise, or not at all; therefore, the final orientation of the segmented vein is not a reliable record of the stretch history of that vein, and their final orientations were not used for determining the distribution of material lines. In addition, establishing the boundary between veins that had only experienced shortening and those that were shortened-then-extended by rotating with the bulk flow (in a dextral sense) was difficult due to the paucity of veins in that orientation ($\sim 345°$ N). Consequently, two possible orientations were chosen for the boundaries between the (s) and (se) sectors, and maximum and minimum Mohr circles were constructed based on these
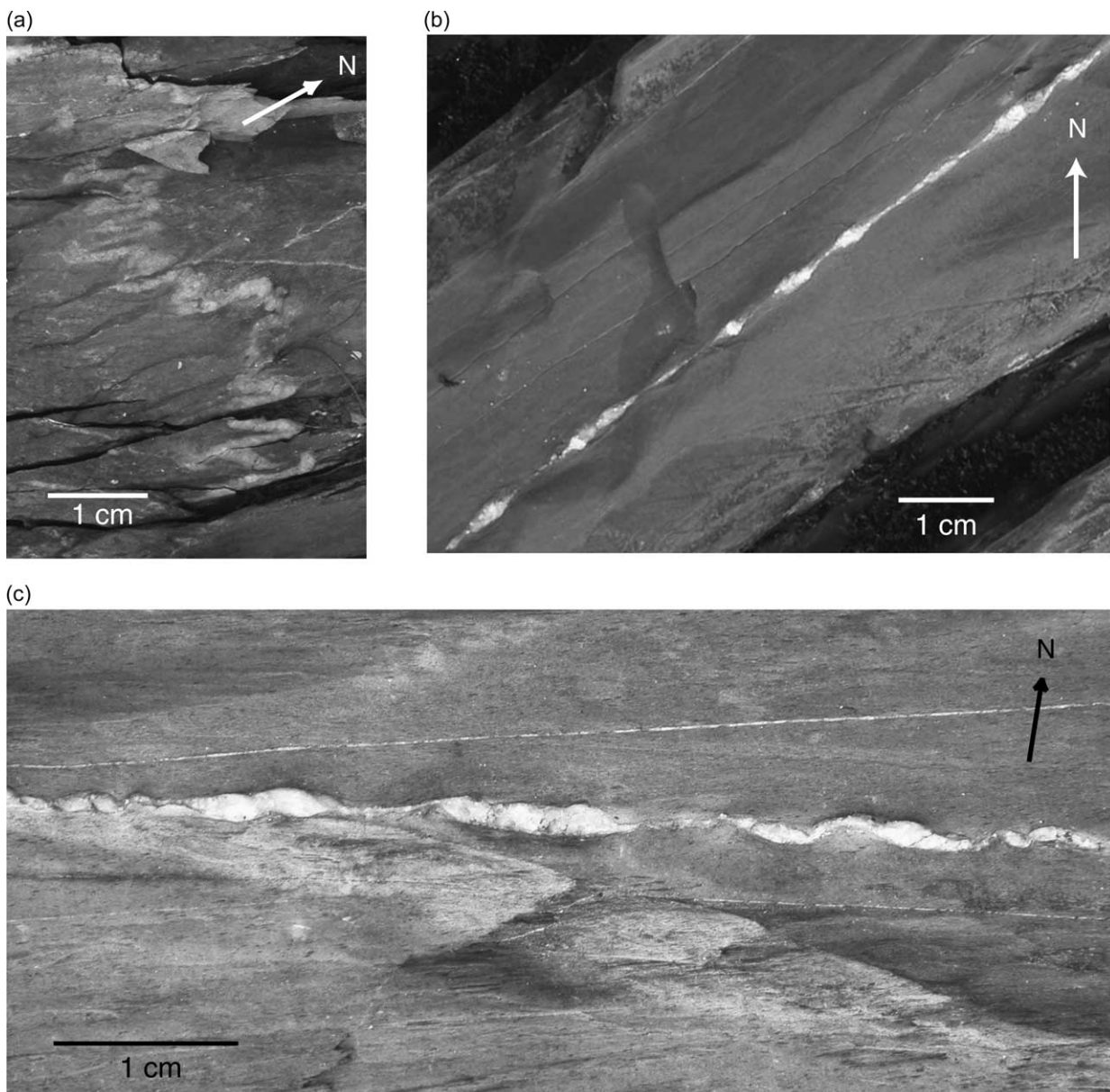

Fig. 10. Photos of veins with different stretch histories used to estimate the vorticity of the D_3 deformation. (a) Shortened vein. (b) Extended vein. (c) Shortened-then-extended vein crossing a quartz-rich layer that is part of an F_2 fold limb.

boundaries. Distinguishing extended veins from veins that have been shortened-then-extended proved difficult in many cases owing to the difficulty of distinguishing tight folds from thick boudins. Another problem occurred with the classification of veins that had been shortened and partially dissolved through pressure solution. Severely buckled veins commonly had the limbs of the folds parallel to the foliation completely dissolved, leaving a series of disjointed fold sections that closely resembled veins that had been first boudinaged, then folded. Inspection of thin sections showed that these are actually folded veins and that they belong in the shortened sector (Fig. 7). A complication of this type of vein morphology is that the spaces between the fold sections are commonly filled with matrix material, and it was difficult to determine if they had yet rotated into the (se) vein sector and had experienced extension. In these cases, the space between the buckled fold sections was closely examined to see if the concentrations of insoluble material left from the pressure solution had experienced extension or not. Once veins were measured and assigned to stretch history sectors, their orientations were plotted as vectors from a central point. Boundaries between the sectors of veins with similar stretch histories were drawn as lines from the central point to positions on the perimeter between clusters of material line points with different stretch histories (Fig. 9).

4.3.1. Coincidence with lines of no instantaneous stretching

Several factors complicate the categorization and interpretation of deformed veins with different stretch histories, causing the boundaries between sectors with different stretch histories *not* to coincide with the lines of no instantaneous stretching. There is some overlap of extended veins into the shortened-then-extended vein sectors. This is probably because in some (se) veins, a certain amount of initial shortening was accommodated by thickening of the vein that is not easily recognized later. All veins identified as extended-only that plot in the se-sectors occur close to the boundaries with the e-sector, lending support to this explanation. The competency contrast between the vein and matrix can influence the behavior of deforming veins as they pass through the se-sector. If there is a high competency contrast, veins may unfold when passing from the shortening to the extension sector resulting in artificially narrow se-sectors from the measured veins. In the case of a small competency contrast between veins and matrix, veins can take up a certain amount of longitudinal shortening or extension after they pass a sector boundary and before they begin to buckle or boudinage (Passchier, 1990a). Competency or viscosity contrast between veins and matrix can be estimated by calculating the wavelength to vein thickness ratio of buckled veins (Ramsay and Huber, 1983). A wavelength to thickness ratio below ∼8 is considered a low to moderate contrast (Wallis, 1992), and for rocks in this study, this ratio ranges from 2.0 to 6.9. A low to moderate viscosity contrast for these veins and matrix is consistent with the above observation that some veins accommodated some shortening without folding, and with the general style of boudinage (Fig. 10). Most importantly, the competency contrast is low enough so that the unfolding of veins as they passed from the s-sector to

the e-sector probably did not occur to a significant extent, so it is likely that the boundaries of the deformed line sectors coincide closely with the two lines of zero instantaneous shortening during the final increment of deformation (Passchier, 1990a; Wallis, 1992). A correction for the positions of the boundaries between material line sectors can be calculated from a known competency contrast, but the influence of competency contrast on sector boundary positions is probably not significant in materials with a low to moderate contrast (Passchier, 1990a), and was not attempted here. Due to layer-parallel shortening and extension during most progressive deformations, shortened, extended, and shortened-then-extended lines will not retain their precise orientations obtained from the deformation being reconstructed through this analysis. Therefore sectors of folded, boudinaged, and folded-then-boudinaged veins will not necessarily coincide precisely with s, e, and se-sectors (Passchier, 1990b). Considering the common occurrence of pressure solution along S_3 foliation in this area, the effect of volume change on the distribution of deformed veins may cause an overestimation of the pure shear component.

4.3.2. The Mohr circle for the position gradient tensor **H**

Any given finite deformation state found in a rock outcrop could have developed through a variety of progressive deformation paths and/or by any sequence of different flow types. However, for each finite deformation there can be one designated eigen flow type, or a flow that would produce the given finite deformation if it had accumulated by steady state flow (Passchier, 1990a,b). Even though most finite deformations in nature do not follow an ideal eigen deformation path (i.e. flow parameters commonly change during progressive deformation), it can be used as an approximation of a standard setting with which flow parameters can be estimated for more realistic deformations. An easy way to obtain the parameters of flow for an eigen-type deformation is by using a Mohr circle for the position gradient tensor **H** (Passchier, 1990a; Wallis, 1992). Material line sectors with different stretch histories are separated by material lines that correspond to lines of no instantaneous longitudinal strain at the onset of deformation and at the last increment of deformation. Passchier (1990a,b) calls these lines *L*-axes, and uses the notation *La* (after deformation) and *Lb* (before deformation) to distinguish between them, and the same terminology will be used here. Because sectors of shortened-then-extended veins form during progressive deformation as veins rotate from the shortening to the extension fields, *La*-axes always separate the s and se sectors, and *Lb* axes always separate the se and e sectors (Fig. 9). These lines are important to distinguish because their positions in real space are used to construct the Mohr circle, and their determination is a critical first step. Next, a Mohr circle of arbitrary size is drawn, and the points La_1, La_2, Lb_1, and Lb_2 are plotted on the perimeter using double the angles between the corresponding lines in real space (Fig. 9), in such a way that the La_1–La_2 line is vertical (Fig. 11). Tie lines are drawn between La_1–Lb_2 and La_2–Lb_1, and normals to those lines from the Lb points are constructed to the left, outside of

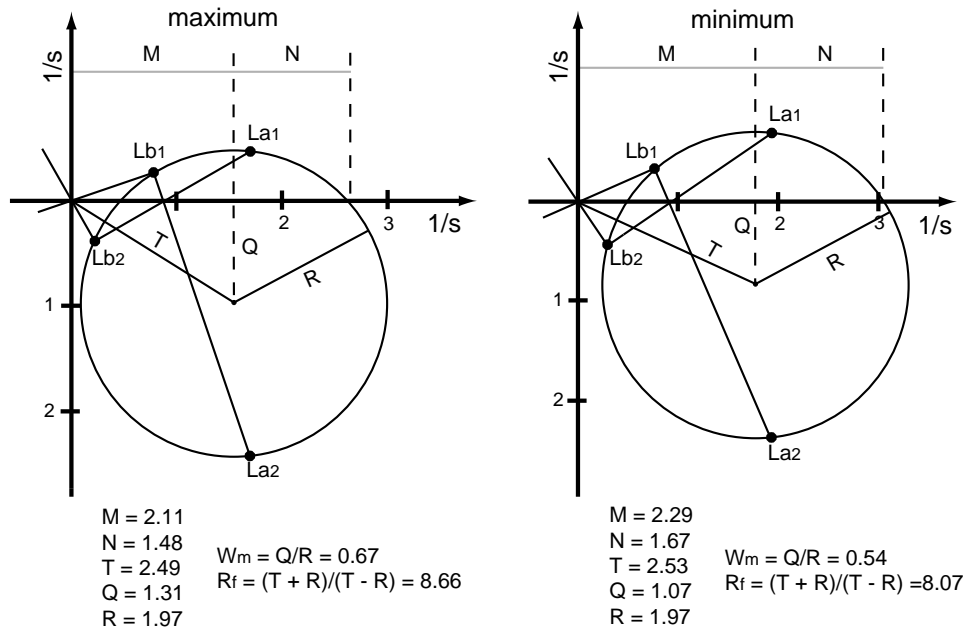Fig. 11. Maximum and minimum Mohr circles for the position gradient tensor **H** constructed from the distribution of deformed lines with different stretch histories (Fig. 9). The values of T, Q, R, M, and N were used to calculate the parameters of flow for the D_3 deformation. The maximum circle is preferred because it is supported by shear strain values calculated from angular shear measurements in both the limestone and quartz-phyllite layers.

the circle. The origin of the Mohr space is where these two lines intersect (Passchier, 1990a). Horizontal and vertical reference axes can then be drawn through the origin, and the scale of the diagram is calculated using the angle between La_1 and La_2 and ratios that are read from the Mohr circle (see Passchier (1990a) for a full explanation of the scale calculations).

4.3.3. Results

The distribution of deformed veins shows two sectors of shortened-then-extended veins (Fig. 9), the N–NE-trending sector being almost four times the size of the ∼E-trending sector, which indicates a general shear deformation with a dextral sense (Passchier, 1990a,b; Passchier and Trouw, 1996). The N–NE-trending sector is larger because it represents veins that rotated from the s sector into the e sector in a clockwise or dextral sense, with the bulk flow. Veins in the ∼E-trending se sector were shortened in an initial orientation such that they rotated in an anti-clockwise or sinistral sense, against the bulk flow, and therefore there are fewer of them (Ghosh and Ramberg, 1976; Passchier, 1990a). The size of the shortened sector, or the angle between La_1 and La_2, is ∼84°, which indicates a slight area increase in the plane of observation, consistent with the continued injection of vein material into the rock. The extension sector lies between Lb_1 and Lb_2, and contains the extensional finite stretching axis and the extensional flow apophysis.

Values for finite deformation parameters read or calculated from the maximum and minimum Mohr circles are: the mean vorticity number, $W_m = 0.67_{max}$, 0.54_{min}; finite strain ratio, $R_f = 8.66_{max}$, 8.073_{min}; the kinematic dilatancy number, $A = 0.1045$; area change in the plane of observation, $1 + \Delta A = 0.175$, and the orientation of the principal finite stretching axis,

$\phi = 37.5°$ using 46° as the orientation of the vein with the largest stretch value. The small positive values for $1 + \Delta A$ and A indicate a small area increase in the plane of observation (Passchier and Urai, 1988; Passchier, 1990a), consistent with vein mineralization in the outcrop. For perspective, if $A < 0$, flow is contracting; if $A > 1$, then all the lines in the rock would be instantaneously extending; so $A = 0.1045$ for this flow indicates a slight deviation from plane strain, but not one significant enough to affect the results of the analysis (Passchier, 1990a). The maximum value of $W_m = 0.67$ for the eigen flow for this finite deformation is favored (see discussion). The finite strain ratio is compatible with the boudinage and buckling observed in outcrop. The orientation of the finite extensional axis $(\phi) = 37.5°$ determined through this method is reasonable within the context of the known orientation of the boundary of the regional shear zone at ∼43° (Osberg et al., 1985).

5. Estimates of shear strain from rotations of fibrous veins

To provide an independent check on the flow parameters determined in the above analysis, the angular shear in both the quartz-phyllite and limestone layers was measured and used to estimate the amount of shear strain using the relationship $\gamma = \tan(\psi)$. Attempts to measure the non-coaxiality of a deformation, W_m, using the principal strains determined from natural gages in the rock and the amount of rotation of rigid equant grains to passive linear markers have been met with reasonable success (e.g. Ghosh and Ramberg, 1976; Ghosh, 1987; Holcomb and Little, 2001; Ghosh et al., 2003). Preliminary analysis of the fibrous calcite veins in boudin necks from the Winslow outcrop indicated that these veins behaved more as passive markers in a non-coaxial flow than as rigid objects.

Independent estimates for the flow parameters during the D_3 deformation are calculated here using the amount of rotation of extended linear veins in limestone, and the undeformed larger-axial-ratio fibrous calcite veins in boudin necks. Over 100 fibrous veins in boudin necks were chosen for analysis based on several criteria: (1) their fibers must be perpendicular to vein walls to ensure initial parallelism with compositional layering, (2) they must have a large axial ratio for these veins, and (3) they must not be visibly affected by later deformation associated with the F_3 asymmetric folds. The angular shear (ψ) was measured in the boudinaged quartz-phyllite layers from a line perpendicular to compositional layering, to the long axis of the fiber vein (Fig. 12) under the assumption that the veins initiated with long axes perpendicular to compositional layering (see Section 3.2). Angular shear was measured in the same manner in the limestone layers. To ensure that only veins with their initial orientations perpendicular to bedding were measured, only the eight linear, extended veins that spanned entire limestone layers and could be visually back-rotated to initial positions by restoring adjacent folded foliation were used. The results are only qualitative, but still provide useful limits on the shear strain and flow parameters in the rock. Shear strain (γ) was calculated for each measured vein through the relationship $\gamma = \tan(\psi)$, and averaged for each rock type. The average shear strain recorded in quartz-phyllite layers is 1.4, and the average shear strain recorded by limestone layers is 2.1, consistent with refraction of vein orientations across bedding interfaces, as well as strain partitioning between the two rock types.

6. Discussion

Analysis of the distribution of deformed veins in limestone with similar stretch histories is both a qualitative and quantitative measure of the sense and vorticity of flow. The asymmetry of the sectors of shortened-then-elongated veins (se) requires that a dextral general shear deformation affected this area. From the Mohr circle for the position gradient tensor **H** constructed using the maximum positions of the *La* lines (see Fig. 11), $W_m = 0.67$ and $R_f = 8.66$, requiring that a shear strain of ~ 1.9 occurred in the limestone layers during the D_3 deformation that produced the distribution of deformed lines analyzed in this study. From the Mohr circle constructed from the minimum positions of the *La* lines, the W_m and R_f values are such that a shear strain of ~ 1.3 would be expected for the limestone layers. The average shear strain calculated in the quartz-phyllite layers is $\gamma = 1.4$. Boudinage and subsequent folding of the boudin segments around rotated fiber veins clearly show that these layers were strong relative to the stretched and strongly foliated limestone layers. Therefore, the shear strain calculated from the minimum positions of the *La* lines is inconsistent with the strain recorded in the more competent phyllite units. The flow parameters and shear strain calculated from the Mohr circle for **H** using the maximum
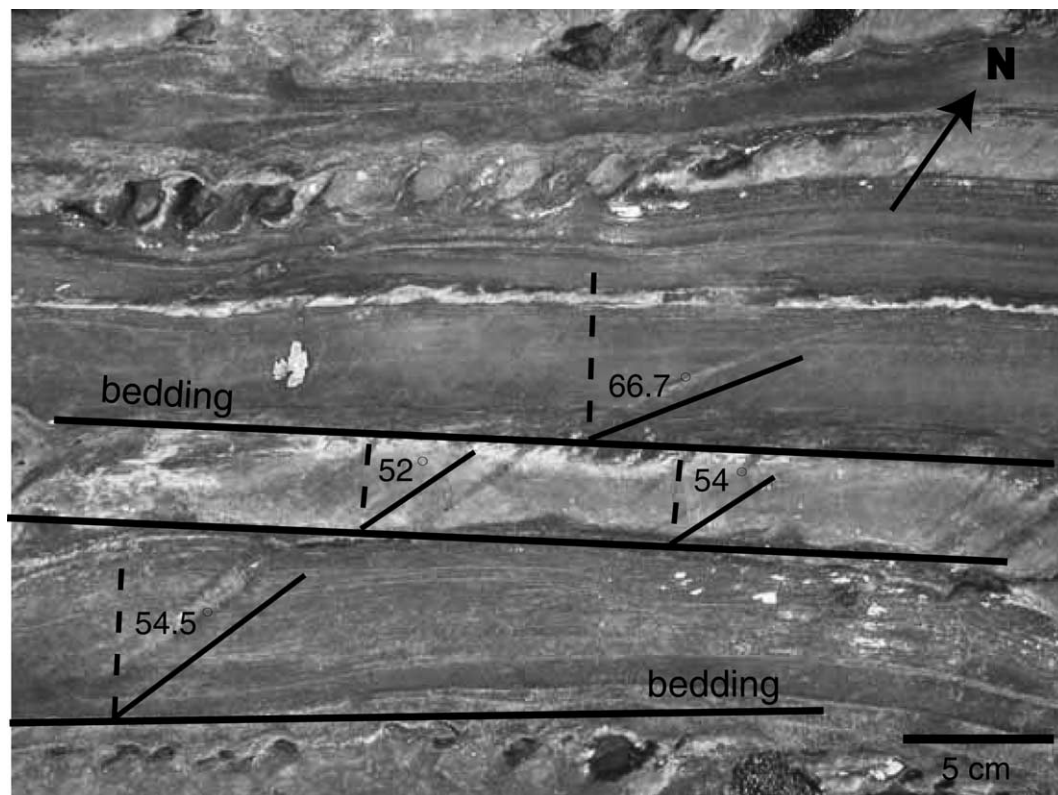

Fig. 12. Measurement of angular shear in quartz-phyllite and limestone layers. Bedding was approximated, and the angle of rotation of the vein was measured from a line perpendicular to bedding (dashed). Note the heterogeneity of the boudinage and extension of the quartz-phyllite layers.

values for the *La* line positions are much more realistic values for this deformation because its shear strain of $\gamma = 1.9$ is supported by the independent qualitative strain analysis of veins in the limestone ($\gamma = 2.1$). In summary, the maximum Mohr circle solution gives a shear strain that falls between those measured in the two rock layers, whereas the minimum Mohr circle solution gives a shear strain less than that measured in the competent layers.

At the Winslow outcrop, ~ 0.25 mm long biotite laths overgrow the S_2 and S_3 foliations in the quartz-phyllite and quartz-mica phyllite layers, but appear deformed by a late, diffuse, and local crenulation cleavage only present around the hinges of S_3 boudin neck vein flanking folds at the thin section scale (Fig. 13). This cleavage is oriented in a $\sim$N–S direction parallel with the fold axes, commonly fans around the folds, and is related to late tightening of the flanking folds. Biotite grew at least by the time of peak Devonian metamorphism of the area at ~ 380 Ma (Osberg, 1988; Tucker et al., 2001); however, recent geochronological studies suggest that regional metamorphism could have begun in this area as early as 400 Ma. Osberg (1988) and Tucker et al. (2001) reported that porphyroblasts overgrow S_3 structures south of the present study area, though it is not clear whether the structures cited correlate with the earlier S_3 foliation or later N–S cleavage of this study. N–S-trending late cleavage is present in dikes in the present study area, and correlative dikes have been dated to 399 ± 1 Ma on the south side of the Kennebec River in Waterville (Tucker et al., 2001). Consequently, the non-coaxial

D_3 deformation responsible for the formation of S_3 through the reactivation of S_2, and the deformation and rotation of fibrous calcite veins at Winslow was active by approximately 399 Ma. Recent work has suggested that mid-Paleozoic deformation in eastern central Maine and northeastern Canada was partitioned into widespread ductile dextral deformation and discrete strike-slip faults at some time after contractional deformation had occurred (Kirkwood, 1995; West and Hubbard, 1997; West et al., 2003). The analysis here demonstrates that a dextral general shear deformation with a significant component of simple shear was present by at least the early-middle Devonian (~ 399 Ma). Re-activation of S_2 foliation by the dextral non-coaxial S_3 foliation could be interpreted as a transition between an orogen-perpendicular and a transpressive tectonic regime, either temporally or spatially or both. However, the observations are also consistent with large-scale strain partitioning in a transpressive orogen (Little et al., 2002; Koons et al., 2003). The outcrop of Waterville Formation at Winslow is located within the broad regional dextral–ductile shear zone associated with the dextral Norumbega fault system, and the structural relationships observed in it may reflect the partitioning of dextral shear strain into the belt of higher-grade rocks to the east, with the pure shear component accommodated by the upright folds and high-angle faults within the larger transpressive orogen (Fig. 1) (West and Hubbard, 1997; Little et al., 2002; Koons et al., 2003). Highly localized orogen-parallel deformation such as the Norumbega fault system would also result from the partitioning of strain in
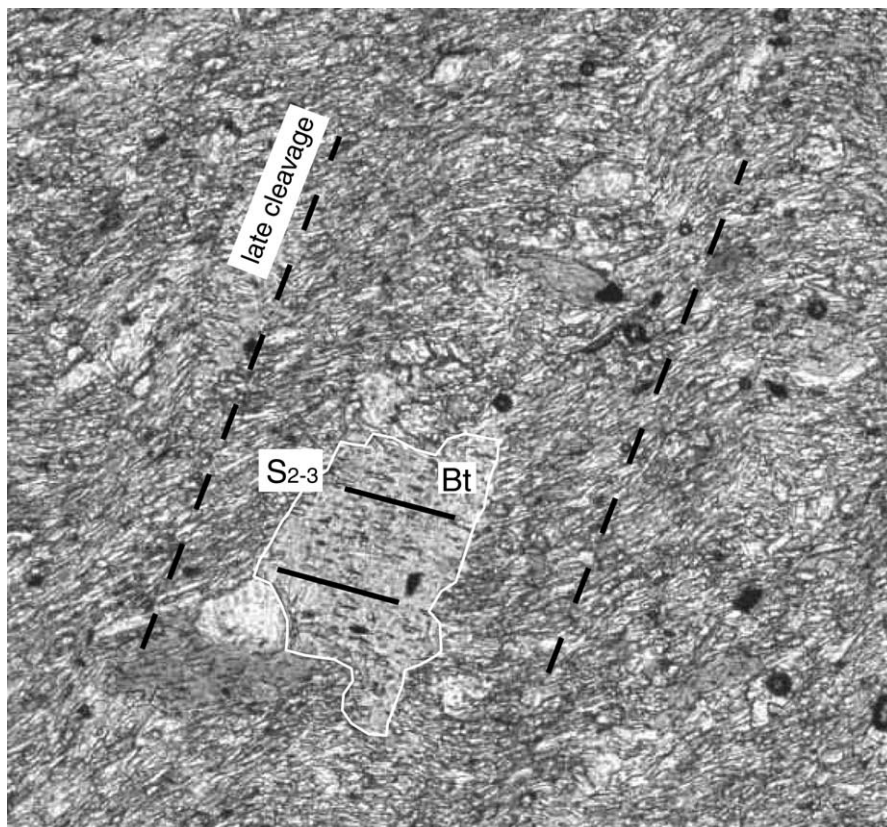

Fig. 13. Photomicrograph of biotite overgrowing S_3 foliation (black lines) in a flanking fold adjacent to a boudin-neck fiber vein.

the context of a transpressional orogen. The sequence of regional deformation phases for eastern central Maine determined in this study is summarized in Table 1.

7. Conclusion

NE-striking S_3 foliation and the NNE-trending asymmetric F_3 folds and cleavage represent two aspects of the same progressive non-coaxial deformation, the asymmetric folds having been generated as shear folds with axes initially parallel to the maximum instantaneous extensional axis ($\sim$N–S), and rotating in a dextral sense through time. D_3 structures and deformed calcite veins preserved in the Waterville Formation unequivocally demonstrate that a transpressive tectonic regime existed by the early-mid Devonian in eastern central Maine. A best estimate for the mean vorticity of this progressive deformation from the distribution of deformed calcite veins with different stretch histories is $W_m = 0.67$, which is supported by independent estimates of the shear strain in the limestone layers. The main phase of this deformation began by at least 399 Ma, constrained by cross-cutting relationships between D_3 fabrics and dikes, and overprinting by the latest regional metamorphism. A model of partitioned dominantly coaxial and dextral non-coaxial strain in a transpressional context is most appropriate for mid-Paleozoic orogenesis in eastern central Maine.

References

Bailey, C.M., Eyster, E.L., 2003. General shear deformation in the Pinaleño Mountains metamorphic core complex, Arizona. Journal of Structural Geology 25, 1883–1892.

Bickle, M.J., Chapman, H.J., Ferry, J.M., Rumble III., D., Fallick, A.E., 1997. Fluid flow and diffusion in the Waterville Limestone, south-central Maine: constraints from strontium, oxygen, and carbon isotope profiles. Journal of Petrology 38 (11), 1489–1512.

Bons, P.D., 2000. The formation of veins and their microstructures. In: Jessell, M.W., Urai, J.L. (Eds.), Stress, Strain and Structure—A Volume in Honour of W.D. Means. Journal of the Virtual Explorer 2.

Bons, P.D., Montenari, M., 2005. The formation of antitaxial calcite veins with well-developed fibres, Oppaminda Creek, South Australia. Journal of Structural Geology 27, 231–248.

Burkhard, M., 1993. Calcite twins, their geometry, appearance and significance as stress strain markers and indicators of tectonic regime: a review. Journal of Structural Geology 15, 351–368.

De Paor, D.G., 1983. Orthographic analysis of geological structures, I. Deformation theory. Journal of Structural Geology 5, 255–278.

Durney, D.W., Ramsay, J.G., 1973. Incremental strains measured by syntectonic crystal growths. In: De Jong, K.A., Scholten, K. (Eds.), Gravity and Tectonics. John Wiley & Sons, New York, pp. 67–96.

Engelder, T., 1987. Joints and shear fractures in rock. In: Atkinson, B.K. (Ed.), Fracture Mechanisms of Rock. Academic Press, London, pp. 27–69.

Ghosh, S.K., 1987. Measure of non-coaxiality. Journal of Structural Geology 9, 111–114.

Ghosh, S.K., Ramberg, H., 1976. Reorientation of inclusions by combination of pure shear and simples shear. Tectonophysics 34, 1–70.

Ghosh, S.K., Sen, G., Sengupta, S., 2003. Rotation of long tectonic clasts in transpressional shear zones. Journal of Structural Geology 25, 1038–1096.

Hilgers, C., Urai, J.L., 2002. Microstructural observations on natural syntectonic fibrous veins: implications for the growth process. Tectonophysics 352, 257–274.

Holcomb, R.J., Little, T.A., 2001. A sensitive vorticity gauge using rotated porphyroblasts, and its application to rocks adjacent to the Alpine Fault, New Zealand. Journal of Structural Geology 23, 979–989.

Kirkwood, D., 1995. Strain partitioning and progressive deformation history of a transpressive belt, northern Appalachians. Tectonophysics 241, 15–35.

Koons, P.O., Norris, R.J., Craw, D., Cooper, A.F., 2003. Influence of exhumation on the structural evolution of transpressional plate boundaries: an example from the Southern Alps, New Zealand. Geology 31 (1), 3–6.

Lister, G.S., Williams, P.F. 1983. The partitioning of deformation in flowing rock masses. Tectonophysics 92, 1–33.

Little, T.A., Holcombe, R.J., Ilg, B.R. 2002. Kinematics of oblique collision and ramping inferred from microstructures and strain in middle crustal rocks, central Southern Alps, New Zealand. Journal of Structural Geology 24: 219–239.

Means, W.D., 1982. An unfamiliar Mohr construction for finite strain. Tectonophysics 4 (89), T1–T6.

Means, W.D., Li, T., 2001. A laboratory simulation of fibrous veins: some first observations. Journal of Structural Geology 23, 857–863.

Means, W.D., Hobbs, B.E., Lister, G.S., Williams, P.F., 1980. Vorticity and non coaxiality in progressive deformation. Journal of Structural Geology 2, 371–378.

Osberg, P.H., 1968. Stratigraphy, structural geology, and metamorphism of the Waterville–Vassalboro area, Maine. Maine Geological Survey Bulletin 20, 64.

Osberg, P.H., 1988. Geologic relations within the shale-wacke sequence in south-central Maine. In: Tucker, R.D., Marvinney, R.G. (Eds.), Studies in Maine Geology Maine Geological Survey, Vol. 1, pp. 51–73.

Osberg, P.H., Hussey, A.M., II, Boone, G.M. (Eds.), 1985. Bedrock Geologic Map of Maine. Maine Geological Survey, Scale = 1:500,000.

Passchier, C.W., 1986. Flow in natural shear zones: the consequences of spinning flow regimes. Earth and Planetary Science Letters 77, 70–80.

Passchier, C.W., 1987. Stable positions of rigid objects in non-coaxial flow: a study in vorticity analysis. Journal of Structural Geology 9, 679–690.

Passchier, C.W., 1988. The use of Mohr circles to describe non-coaxial progressive deformation. Tectonophysics 149, 323–338.

Passchier, C.W., 1990a. Reconstruction of deformation and flow parameters from deformed veins sets. Tectonophysics 180, 185–199.

Passchier, C.W., 1990b. A Mohr circle construction to plot the stretch history of material lines. Journal of Structural Geology 12, 513–515.

Passchier, C.W., 2001. Flanking structures. Journal of Structural Geology 23, 951–962.

Passchier, C.W., Trouw, R.A.J., 1996. Microtectonics. Springer-Verlag, Berlin, Heidelburg. 289pp.

Passchier, C.W., Urai, J.L., 1988. Vorticity and strain analysis using Mohr diagrams. Journal of Structural Geology 10 (7), 755–763.

Ramberg, H., 1975. Particle paths, displacement and progressive strain applicable to rocks. Tectonophysics 28, 1173–1187.

Ramsay, J.G., Huber, M.I., 1983. The Techniques of Modern Structural Geology, Volume 1: Strain Analysis. Academic Press, London. 307pp.

Simpson, C., De Paor, D.G., 1993. Strain and kinematic analysis in general shear zones. Journal of Structural Geology 15, 1–20.

Simpson, C., De Paor, D.G., 1997. Practical analysis of general shear zones using the porphyroclast hyperbolic distribution method: an example from the Scandinavian Caledonides. In: Sengupta, S. (Ed.), Evolution of Geological Structures in Micro- to Macro- Scales. Chapman and Hall, pp. 169–184.

Talbot, C.J., 1970. The minimum strain ellipsoid using deformed quartz veins. Tectonophysics 9, 46–76.

Tikoff, B., Teyssier, C., 1994. Strain and fabric analyses based on porphyroclast interaction. Journal of Structural Geology 16, 477–491.

Tucker, R.D., Osberg, P.H., Berry IV., H.N., 2001. The geology of part of Acadia and the nature of the Acadian orogeny across central and eastern Maine. American Journal of Science 301, 205–260.

Vernon, R.H., 1981. Optical microstructure of partly recrystallized calcite in some naturally deformed marbles. Tectonophysics 78, 601–612.

Wallis, S.R., 1992. Vorticity analysis in a metachert from the Sanbagawa belt, SW Japan. Journal of Structural Geology 14, 271–280.

West Jr., D.P., Beal, H.M., Grover, T.W., 2003. Silurian deformation and metamorphism of Ordovician arc rocks of the Casco Bay Group, south-central Maine. Canadian Journal of Earth Sciences 40 (6), 887–905.

West Jr., D.P., Hubbard, M.S., 1997. Progressive localization of deformation during exhumation of a major strike-slip shear zone: Norumbega fault zone, south-central Maine, USA. Tectonophysics 273, 185–201.

Williams, P.F., Urai, J.L., 1989. Curved vein fibres: an alternative explanation. Tectonophysics 158, 311–333.

Wiltschko, D.V., Morse, J.W., 2001. Crystallization pressure versus "crack seal" as a mechanism for banded veins. Geology 29, 79–82.